Signatures of Chaos in Nonintegrable Models of Quantum Field Theories

Miha Srdinšek,* Tomaž Prosen, and Spyros Sotiriadis
Faculty of Mathematics and Physics, University of Ljubljana, Ljubljana SI 1000, Slovenia

(Received 26 January 2021; accepted 25 February 2021; published 22 March 2021)

We study signatures of quantum chaos in $(1+1)$D quantum field theory (QFT) models. Our analysis is based on the method of Hamiltonian truncation, a numerical approach for the construction of low-energy spectra and eigenstates of QFTs that can be considered as perturbations of exactly solvable models. We focus on the double sine-Gordon, also studying the massive sine-Gordon and ϕ^4 model, all of which are nonintegrable and can be studied by this method with sufficiently high precision from small to intermediate perturbation strength. We analyze the statistics of level spacings and of eigenvector components, which are expected to follow random matrix theory predictions. While level spacing statistics are close to the Gaussian orthogonal ensemble (GOE) as expected, on the contrary, the eigenvector components follow a distribution markedly different from the expected Gaussian. Unlike in the typical quantum chaos scenario, the transition of level spacing statistics to chaotic behavior takes place already in the perturbative regime. Moreover, the distribution of eigenvector components does not appear to change or approach Gaussian behavior, even for relatively large perturbations. Our results suggest that these features are independent of the choice of model and basis.

DOI: 10.1103/PhysRevLett.126.121602

Introduction.—The physics of nonintegrable quantum systems has been successfully described by quantum chaos theory, which states that their spectral statistics are given by random matrix theory (RMT), i.e., exhibit the same behavior as matrices whose elements are randomly chosen from a Gaussian distribution. These conjectures [1–3] have been verified for a broad class of single-particle models, where they have been explained in terms of semiclassical periodic orbit theory [4,5]. More recently research focus has shifted to many-body systems [6–16], where RMT predictions have been verified numerically and in certain cases even analytically [17,18]. Chaoticity tests in quantum many-body models are, however, almost exclusively limited to discrete (lattice) models, leaving continuous models unexplored. Among them, relativistic quantum field theories (QFTs) and their dynamics lie at the cornerstone of important open questions of theoretical physics, like the black hole information paradox [19], making the study of ergodicity and chaos in QFT a topic of fundamental interest.

Significant progress in this direction has been made based on new theoretical concepts and indicators [20–22]. Nevertheless, the emergence of quantum chaos in QFT remains poorly understood in terms of the more traditional measures of level spacing and eigenvector statistics [23]. Studying level spacing statistics is the best way of detecting level repulsion, the characteristic property of random matrix spectra. On the other hand, a Gaussian distribution of eigenvector components is an important indication of validity of the eigenstate thermalization hypothesis (ETH) [24,25], which explains how thermalization emerges from the dynamics of nonintegrable quantum systems [26].

The main obstacle in performing chaoticity tests in QFT is that, unlike for lattice models of condensed matter physics, QFT models are continuous and thus live in an infinite dimensional Hilbert space. Therefore, exact computation of energy spectra is not an option for nonintegrable models, and we inevitably resort to approximate numerical methods. The challenge is then to achieve sufficiently high accuracy in a sufficiently large part of the spectrum, so that a statistical analysis is possible and reliable. An ideal method for this task is the "truncated conformal space approach" (TCSA) [27–29], more generally the Hamiltonian truncation method [30,31]. The TCSA is based on the algebraic toolkit of conformal field theory (CFT) and insights from renormalization group theory, which can capture efficiently nonperturbative effects in the low-energy spectrum, and is especially suitable for $(1+1)$D models. A pioneering study of quantum chaos indicators using this method was presented in Ref. [32] for the tricritical and tetracritical Ising field theories, demonstrating that their level spacing statistics agree with the theoretical expectations in both the integrable and nonintegrable case, and observing their crossover for varying parameters.

In this Letter we study two independent and equally important signatures of quantum chaos, the distribution of level spacings as quantified by the consecutive level spacing ratios $\tilde{r}$ [33,34] and the distribution of eigenvector components. We study a class of $(1+1)$D models: the sine-Gordon model (SG), which is integrable, and the double sine-Gordon (DSG), massive sine-Gordon (MSG) a.k.a. Schwinger-Thirring, and ϕ^4 model, which are all

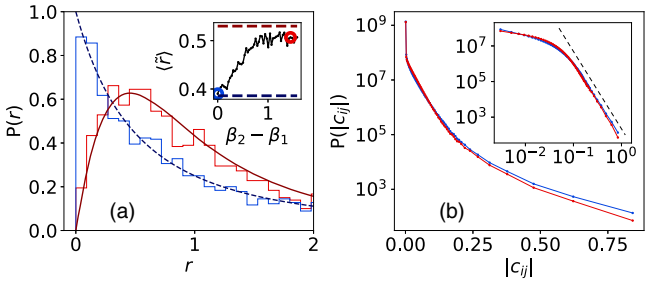

FIG. 1. Statistics of level spacings and eigenvector components in the double sine-Gordon (nonintegrable) and sine-Gordon (integrable) model. (a) Change in the r distribution of DSG from $(\beta_1, \beta_2) = (2.5, 2.5)$ (integrable SG point) to $(\beta_1, \beta_2) = (1.0, 2.5)$ (nonintegrable point) compared to the predictions for integrable models (dashed blue curve) and to the RMT predictions (red curve), respectively. Inset shows change in the average of $\tilde{r}$ when varying β_1. (b) Distribution of the absolute values of eigenvector components $|c_{ij}|$ for the same two points, in log scale and log-log scale (inset). The GOE distribution of $|c_{ij}|$ is Gaussian. Instead, we observe that, although the level spacing statistics of DSG is GOE-like, the statistics of $|c_{ij}|$ is not.

nonintegrable. We verify that level spacings follow the expected Poisson distribution for SG and Gaussian orthogonal ensemble (GOE) distribution for DSG, MSG and ϕ^4 model to a very good approximation. GOE behavior is actually observed already in the weakly perturbed CFT regime, in contrast to what typically happens in single-particle models. Surprisingly, we find that, even when the level spacing distribution is close to GOE, the eigenvector component distribution is markedly different from the Gaussian found in RMT [35] (Fig. 1). On the contrary, it exhibits at best exponential scaling followed by an algebraically decaying tail, which contradicts the RMT prediction. This last feature is robust and independent of the model and parameter values. We validate our observations by pushing the limits of TCSA's potential to achieve high accuracy and devising a reliable measure of truncation error, which is crucial for distinguishing physical behavior from numerical artifacts.

Models, method, and observables.—We consider the following models: the SG with Hamiltonian $H_{\mathrm{SG}} = H_0 + \lambda V_\beta$, the DSG $H_{\mathrm{DSG}} = H_0 + \lambda_1 V_{\beta_1} + \lambda_2 V_{\beta_2}$, the MSG $H_{\mathrm{MSG}} = H_0 + \lambda V_{\beta_1} + m^2 U_2$, and the ϕ^4 model $H_{\phi^4} = H_0 + m^2 U_2 + \lambda U_4$, where

$$H_0 = \frac{1}{2}\int [\pi^2 - (\partial_x \phi)^2] dx,$$
$$U_n = \frac{1}{n!}\int \phi^n dx, \qquad V_\beta = -\int \cos\beta\phi dx. \tag{1}$$

The SG is a prototypical integrable QFT possessing topological excitations [29,36–38] and is equivalent to the massive Thirring model [39,40]. It has applications in condensed matter and atomic physics [41] and has been simulated experimentally [42,43]. The DSG is nonintegrable and also topologically nontrivial [44–47]. Lastly, the MSG is equivalent to the Schwinger-Thirring model, reducing to $(1+1)$D QED at $\beta = \sqrt{4\pi}$ [48,49].

All the above models can be seen as perturbations of the free boson CFT H_0 by relevant operators V and as such they can be studied using TCSA. This method yields numerical approximations of the low-energy spectrum of $H = H_0 + \lambda V$ based on the simple idea of computing the matrix elements of V in an energy-truncated basis $\{|\Phi_n^0\rangle : E_n^0 \leq E_{\mathrm{cut}}\}$ of H_0 and diagonalizing the resulting finite matrix approximation of H. If V does not couple significantly the low- with the high-energy spectrum of H_0, which is true for relevant perturbations, then the numerical spectrum is expected to converge to the exact upon increasing the truncation cutoff E_{cut}. TCSA has been successfully applied to the SG [29,37,38,50,51] and DSG [45,47] and recently also the Schwinger model, a special limit of MSG [52], while a similar Hamiltonian truncation method has been used for the ϕ^4 model [30,53–56].

Using TCSA we compute a low-energy part of the spectra E_n and eigenvectors $|\Phi_n\rangle$ of the above models for various parameter values and analyze their statistics. More specifically, we compute the distributions of level spacings $s_n = E_{n+1} - E_n$, of consecutive level ratios r_n and $\tilde{r}_n$ defined as [33]

$$r_n = s_n / s_{n-1}, \qquad \tilde{r}_n = \min(r_n, 1/r_n) \tag{2}$$

and of eigenvector components $c_{ij} = \langle \Phi_i^0 | \Phi_j \rangle$ in the TCSA basis. Since all models are time-reversal symmetric, the corresponding RMT ensemble is the GOE where the r distribution is $P_{\mathrm{GOE}}(r) \propto (r + r^2)/(1 + r + r^2)^{5/2}$ and that of $\tilde{r}$ is the restriction of the latter to the interval [0, 1], with mean value $\langle \tilde{r} \rangle_{\mathrm{GOE}} \approx 0.536$ [34]. Conversely, in integrable models level spacings follow the Poisson distribution [57] with $\langle \tilde{r} \rangle_P \approx 0.386$. Compared to other tests of level spacing statistics, $\tilde{r}$ has the advantage of being independent of the local level density, therefore no "unfolding" [23] is necessary. For the eigenvector component distribution, the RMT prediction is Gaussian, resulting in the Porter-Thomas distribution for their absolute values [35], while for integrable models it is expected to be algebraic [58].

To minimize numerical errors we use truncated bases much larger than in previous studies (~85000 states at the highest cutoff). Moreover, to ensure our results are sufficiently accurate, we verify convergence using rather strict truncation error estimates, based on measures of their correlations at successive cutoffs (see figure captions and the Supplemental Material [59]).

Level spacing statistics.—We start by analyzing the statistics of r values. Figure 1(a) shows the distribution $P(r)$ for DSG at two different choices of parameter values, one integrable $(\beta_1, \beta_2) = (2.5, 2.5)$ (SG) and one nonintegrable $(\beta_1, \beta_2) = (1.0, 2.5)$. The parameters λ_1, λ_2 have

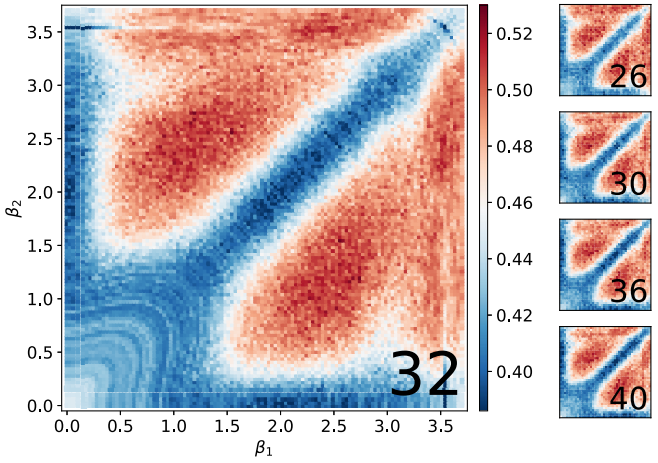

FIG. 2. Density plot of $\langle\tilde{r}\rangle$ in DSG as a function of β_1 and β_2. The model is nonintegrable with the exception of the three lines $\beta_1 = 0$, $\beta_2 = 0$, and $\beta_1 = \beta_2$, where it reduces to the SG. The $\langle\tilde{r}\rangle$ is indeed close to $\langle\tilde{r}\rangle_P$ (dark blue) along the SG lines and in their vicinity, while it approaches $\langle\tilde{r}\rangle_{\mathrm{GOE}}$ (dark red) away from them. Plots for different truncation cutoffs E_{cut} are included for comparison (right). (Parameters: $l_1 = l_2 = 1$, energy window: 1000–3000 levels, E_{cut} reported at the bottom right corner of each plot).

been chosen so that the energy gap between the ground and first excited state is of the same order as the inverse system size L^{-1} (more precisely, $l_1 = l_2 = 1$ where $l_i = m_{\beta_i} L$ and m_β is the SG breather mass [59]). These values are within the perturbative regime where convergence is optimal. We observe that the two distributions agree quite well with the Poisson and GOE distributions, respectively. The change of statistics can be demonstrated by the mean value $\langle\tilde{r}\rangle$ for varying β_1 at fixed β_2 [Fig. 1(a), inset]. Starting from the Poisson value for $\beta_1 = 0$, $\langle\tilde{r}\rangle$ increases towards the GOE value, fluctuating close and below it. The complete dependence of $\langle\tilde{r}\rangle$ on both β_1 and β_2 is shown in Fig. 2 in the form of a "phase diagram." The $\langle\tilde{r}\rangle$ is close to Poisson along the SG lines ($\beta_1 = 0$, $\beta_2 = 0$ and $\beta_1 = \beta_2$), whereas it approaches $\langle\tilde{r}\rangle_{\mathrm{GOE}}$ in the areas away from these lines.

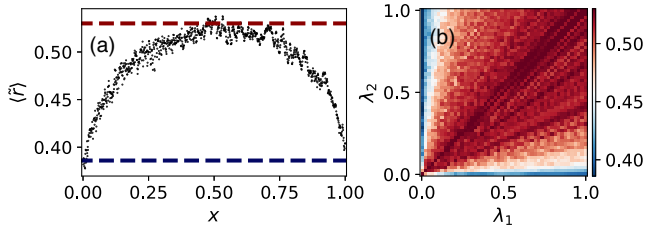

FIG. 3. Dependence of $\langle\tilde{r}\rangle$ on the perturbation strength in DSG. (a) Plot of $\langle\tilde{r}\rangle$ for λ_1, $\lambda_2 \to 0$ as a function of the mixing ratio $x = \lambda_1/(\lambda_1 + \lambda_2)$. (b) Density plot of $\langle\tilde{r}\rangle$ as a function of λ_1 and λ_2. The SG lines correspond to $\lambda_1 = 0$ and $\lambda_2 = 0$. Note that $\langle\tilde{r}\rangle \approx \langle\tilde{r}\rangle_{\mathrm{GOE}}$ even in the immediate vicinity of the unperturbed CFT model. [Parameters: $(\beta_1, \beta_2) = (1, 2.5)$].

By independently varying the perturbation strength parameters λ_1, λ_2 at fixed $(\beta_1, \beta_2) = (1, 2.5)$ (Fig. 3) we find that $\langle\tilde{r}\rangle$ is close to $\langle\tilde{r}\rangle_{\mathrm{GOE}}$ even in the immediate vicinity of the unperturbed CFT model, i.e., for λ_1, $\lambda_2 \to 0$, as long as the ratio λ_1/λ_2 is kept fixed at $\sim$1. This is somewhat surprising given that chaoticity typically emerges far from integrable points and outside the perturbative regime. Chaotic $\langle\tilde{r}\rangle$ values can indeed be verified from first-order perturbation theory results [Fig. 3(a)] [59]. The fluctuations of $\langle\tilde{r}\rangle$ can be partially attributed to the relatively small energy window (2000 levels), as random matrices of the same size display similar fluctuations. Nevertheless, we notice that $\langle\tilde{r}\rangle$ is predominantly below $\langle\tilde{r}\rangle_{\mathrm{GOE}}$, meaning that this is still a transitional, not completely chaotic behavior.

The differences between $\langle\tilde{r}\rangle$ at different cutoffs (Fig. 2) are negligible, with the best convergence achieved for small β_1, β_2. However, even if $\langle\tilde{r}\rangle$ converges at some cutoff to $\langle\tilde{r}\rangle_{\mathrm{GOE}}$, this does not necessarily mean that this is the correct physical value, since a nonconvergent spectrum is also likely to be RMT-like. For this reason, we check the convergence using an error estimate based on the averaged absolute differences of $\tilde{r}$ values between successive cutoffs and verifying that the error decreases with increasing cutoff [59]. We empirically find that increasing β_i or l_i results in larger truncation errors, making the numerical data less reliable. Moreover, in TCSA convergence is achieved in the lowest part of the computed spectra, with the truncation effects increasing at higher levels. For the parameters of Fig. 1, a sufficiently good level of convergence of r values is achieved for the lowest $\sim$3000 levels at $E_{\mathrm{cut}} = 42$ (in units $\varepsilon = \pi/L$).

Eigenvector statistics.—Let us focus on the statistics of eigenvector components c_{ij} in DSG. Figure 1(b) shows the distribution of their absolute values in log scale for the same choice of parameters as in Fig. 1(a), one exhibiting Poisson and the other GOE level spacing statistics. Despite the clear difference in the latter, the eigenvector distributions are practically the same in both cases and different from the Gaussian prediction of RMT. In the bulk of the distribution the scaling is at best exponential while the tails decay slower, like an algebraic function. This is in strong contrast with theoretical expectations for chaotic models [35]. To eliminate truncation effects, we have again restricted the analysis to the convergent low-energy part of the matrix c_{ij}.

To gain a deeper insight into this observation, we look more closely into the structure of the matrix c_{ij}. Figures 4(a)–4(e) show c_{ij} for DSG at increasing perturbation strength $l = l_1 = l_2$. We observe that for small l, c_{ij} is characterized by an approximately block-diagonal form, which is easily explained by perturbation theory given that the CFT spectrum is organized in degenerate energy shells [59]. For increasing l this block structure fades away and c_{ij} becomes more uniform, even though a pattern of fine structure remains always visible.

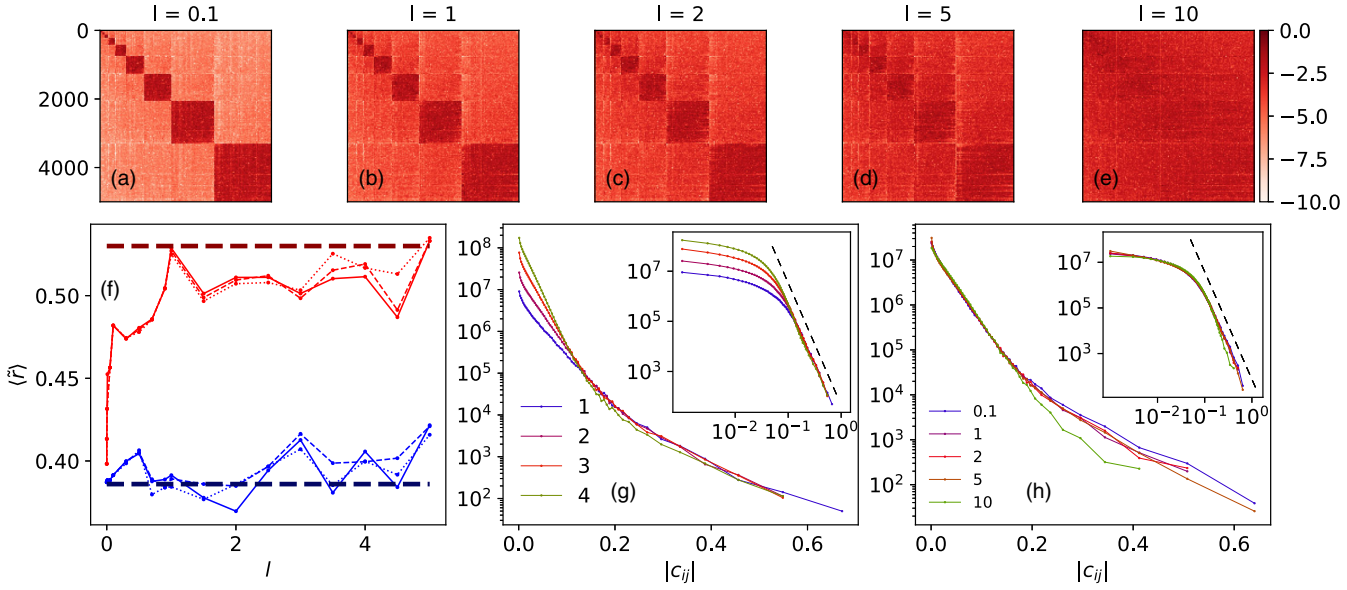

FIG. 4. Dependence of spectral properties on perturbation strength. (a)–(e) Matrix plot of the eigenvector matrix $|c_{ij}|$ of DSG at different $l = l_1 = l_2$, in logarithmic scale. Only the low-energy part (top left corner) of the matrix is shown, which is fully convergent for $l \leq 2$, partially convergent for $l \approx 5$ (lowest ~3000 levels convergent), and poorly convergent for $l \approx 10$. (f) Plot of $\langle\tilde{r}\rangle$ as a function of l at different cutoffs (dotted: 38, dashed: 40, solid line: 42) for DSG (red) and SG (blue). (g) Distributions of $|c_{ij}|$ in the last four boxes shown in (a)–(e), labeled as 1–4. (h) Distribution of $|c_{ij}|$ in the third largest box for different l. [Parameters: $(\beta_1, \beta_2) = (1.0, 2.5)$ for DSG, $\beta = 2.5$ for SG.]

Based on these observations, we analyze how the DSG eigenvector distribution depends on l, whether it approaches the RMT prediction when moving from weak to strong perturbation, and how it changes from one block to another. The distributions inside a single block exhibit clearly exponential scaling in the bulk, still with slower decaying tails [Fig. 4(g)]. The slope of this exponential changes from block to block. The distribution in Fig. 1, which corresponds to a large window including many blocks, is actually a superposition of many exponential distributions. There is no significant change when l increases from 0 to ~5, the maximum value for which we achieved convergence [Fig. 4(h)]. In fact, the distribution remains unchanged even for larger l, where truncation effects are non-negligible. At the same time, $\langle\tilde{r}\rangle \approx \langle\tilde{r}\rangle_{\mathrm{GOE}}$ for any $l \gtrsim 1$ and well convergent at least for $l \lesssim 3$ [Fig. 4(f)].

Comparing the eigenvector statistics of different models in windows with $\langle\tilde{r}\rangle \approx \langle\tilde{r}\rangle_{\mathrm{GOE}}$, we find that they generally vary from model to model but are always different from Gaussian and at best exponential [Fig. 5(b)]. The ϕ^4 model, in particular, deserves special attention. In this case, using the CFT as the unperturbed model to construct the truncation basis is inconvenient, so the massive Klein-Gordon (KG) model $H_{\mathrm{KG}} = H_0 + m^2 U_2$ is used instead [30]. In contrast to the CFT basis, in KG there is no degenerate shell structure. Nevertheless, the eigenvector distribution is once again very different from Gaussian and characterized by slowly decaying tails as in DSG. Lastly, comparing the single-block eigenvector distributions in SG at different β [Fig. 5(a)], we find that they are similar to those of DSG. These results clearly show that the discrepancy between the eigenvector distributions and RMT prediction, in particular the presence of slowly decaying tails, is robust under variations of the parameters, energy window, model and truncation basis.

Discussion.—We have shown that, while the level spacing statistics of the above studied nonintegrable QFTs agree with RMT, their eigenvector component

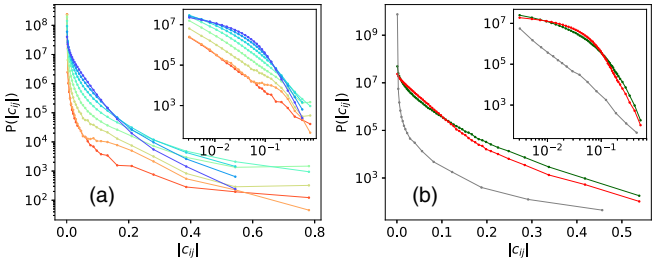

FIG. 5. (a) Distribution of $|c_{ij}|$ in SG in log and log-log scale (inset) at different β from 0 (red) to 2.5 (blue). The exponential scaling in the bulk is not a special property of the non-integrable DSG but is also present in SG. (b) Comparison of $|c_{ij}|$ distributions in DSG (red), MSG (green), and ϕ^4 model (gray), always in windows with GOE spectral statistics. Even though the ϕ^4 model is expanded in a different and less exceptional basis (KG), the distribution is still not GOE-like but clearly algebraic. [Model parameters, $\langle\tilde{r}\rangle$ values: DSG: $(\beta_1, \beta_2) = (1.0, 2.5)$, $l = 1$, MSG: $\beta = 2.8$, $m = 0.76$, $l = 1$ $(\langle\tilde{r}\rangle = 0.519)$, ϕ^4: $\lambda = 1.0$, $m = 1$, $L = 7$ $(\langle\tilde{r}\rangle = 0.5)$].

statistics are markedly different from RMT predictions. Both of the above features emerge already in the weakly perturbed CFT regime and persist unchanged beyond that, which suggests that they may be valid for any perturbation strength. Indeed, there is no indication that the scaling of the distributions changes with the perturbation, even when the CFT shell structure disappears. Moreover, the qualitative characteristics of the eigenvector distributions for different models are similar, irrespective of integrability and even for quite different choices of truncation basis. The latter observation particularly rules out an explanation based on exceptional features of the CFT basis. An interesting open question is how the observed discrepancy affects the validity of ETH in $(1+1)$D QFT. Testing ETH using Hamiltonian truncation methods is, however, a more challenging problem, as it is supposed to hold in the thermodynamic limit where the perturbation strength is large and convergence of the spectra worsens. We hope to investigate this question in the future.

The data presented in this work may be accessed in Ref. [60].

The authors would like to thank Ivan Kukuljan for collaboration and assistance with programming at an early stage of this project. S. S. would also like to thank Gabor Takács and Robert Konik for useful discussions. M. S. and S. S. acknowledge support by the Slovenian Research Agency (ARRS) under the Grant No. QTE (N1-0109). T. P. acknowledges support by the ERC Advanced Grant 694544—OMNES and the ARRS research program P1-0402.

*Corresponding author.
miha.srdinsek@sorbonne-universite.fr

[1] G. Casati, F. Valz-Gris, and I. Guarnieri, Lett. Nuovo Cimento **28**, 279 (1980).
[2] O. Bohigas, M. J. Giannoni, and C. Schmit, Phys. Rev. Lett. **52**, 1 (1984).
[3] M. V. Berry, J. Phys. A **10**, 2083 (1977).
[4] E. B. Bogomolny, Physica (Amsterdam) **31D**, 169 (1988).
[5] S. Müller, S. Heusler, P. Braun, F. Haake, and A. Altland, Phys. Rev. Lett. **93**, 014103 (2004).
[6] L. F. Santos and M. Rigol, Phys. Rev. E **81**, 036206 (2010).
[7] L. F. Santos and M. Rigol, Phys. Rev. E **82**, 031130 (2010).
[8] M. Rigol and L. F. Santos, Phys. Rev. A **82**, 011604(R) (2010).
[9] L. D'Alessio, Y. Kafri, A. Polkovnikov, and M. Rigol, Adv. Phys. **65**, 239 (2016).
[10] V. Alba, Phys. Rev. B **91**, 155123 (2015).
[11] W. Beugeling, R. Moessner, and M. Haque, Phys. Rev. E **91**, 012144 (2015).
[12] W. Beugeling, A. Bäcker, R. Moessner, and M. Haque, Phys. Rev. E **98**, 022204 (2018).
[13] W. Beugeling, A. Andreanov, and M. Haque, J. Stat. Mech. (2015) P02002.
[14] M. Haque, P. A. McClarty, and I. M. Khaymovich, arXiv:2008.12782.
[15] L. Foini and J. Kurchan, Phys. Rev. Lett. **123**, 260601 (2019).
[16] A. Chan, A. De Luca, and J. T. Chalker, Phys. Rev. X **8**, 041019 (2018).
[17] P. Kos, M. Ljubotina, and T. Prosen, Phys. Rev. X **8**, 021062 (2018).
[18] B. Bertini, P. Kos, and T. Prosen, Phys. Rev. Lett. **121**, 264101 (2018).
[19] P. Hayden and J. Preskill, J. High Energy Phys. 09 (2007) 120.
[20] Y. Sekino and L. Susskind, J. High Energy Phys. 10 (2008) 065.
[21] S. H. Shenker and D. Stanford, J. High Energy Phys. 03 (2014) 067.
[22] J. Maldacena, S. H. Shenker, and D. Stanford, J. High Energy Phys. 08 (2016) 106.
[23] F. Haake, *Quantum Signatures of Chaos* (Springer, Berlin, Heidelberg, 2010).
[24] J. M. Deutsch, Phys. Rev. A **43**, 2046 (1991).
[25] M. Srednicki, J. Phys. A **32**, 1163 (1999).
[26] S. Hortikar and M. Srednicki, Phys. Rev. E **57**, 7313 (1998).
[27] V. P. Yurov and A. B. Zamolodchikov, Int. J. Mod. Phys. A **05**, 3221 (1990).
[28] V. P. Yurov and A. B. Zamolodchikov, Int. J. Mod. Phys. A **06**, 4557 (1991).
[29] G. Feverati, F. Ravanini, and G. Takács, Phys. Lett. B **430**, 264 (1998).
[30] M. Hogervorst, S. Rychkov, and B. C. van Rees, Phys. Rev. D **91**, 025005 (2015).
[31] A. J. A. James, R. M. Konik, P. Lecheminant, N. J. Robinson, and A. M. Tsvelik, Rep. Prog. Phys. **81**, 046002 (2018).
[32] G. P. Brandino, R. M. Konik, and G. Mussardo, J. Stat. Mech. (2010) P07013.
[33] V. Oganesyan and D. A. Huse, Phys. Rev. B **75**, 155111 (2007).
[34] Y. Y. Atas, E. Bogomolny, O. Giraud, and G. Roux, Phys. Rev. Lett. **110**, 084101 (2013).
[35] T. A. Brody, J. Flores, J. B. French, P. A. Mello, A. Pandey, and S. S. M. Wong, Rev. Mod. Phys. **53**, 385 (1981).
[36] A. B. Zamolodchikov, Int. J. Mod. Phys. A **10**, 1125 (1995).
[37] G. Feverati, F. Ravanini, and G. Takács, Nucl. Phys. **B540**, 543 (1999).
[38] G. Fehér and G. Takács, Nucl. Phys. **B852**, 441 (2011).
[39] S. Coleman, Phys. Rev. D **11**, 2088 (1975).
[40] S. Mandelstam, Phys. Rev. D **11**, 3026 (1975).
[41] T. Giamarchi, *Quantum Physics in One Dimension* (Oxford University Press, Oxford, 2004).
[42] T. Schweigler, V. Kasper, S. Erne, I. Mazets, B. Rauer, F. Cataldini, T. Langen, T. Gasenzer, J. Berges, and J. Schmiedmayer, Nature (London) **545**, 323 (2017).
[43] T. V. Zache, T. Schweigler, S. Erne, J. Schmiedmayer, and J. Berges, Phys. Rev. X **10**, 011020 (2020).
[44] G. Delfino and G. Mussardo, Nucl. Phys. **B516**, 675 (1998).
[45] Z. Bajnok, L. Palla, G. Takács, and F. Wágner, Nucl. Phys. **B601**, 503 (2001).
[46] G. Mussardo, V. Riva, and G. Sotkov, Nucl. Phys. **B687**, 189 (2004).

[47] G. Takács and F. Wágner, Nucl. Phys. **B741**, 353 (2006).
[48] S. Coleman, R. Jackiw, and L. Susskind, Ann. Phys. (N.Y.) **93**, 267 (1975).
[49] S. Coleman, Ann. Phys. (N.Y.) **101**, 239 (1976).
[50] I. Kukuljan, S. Sotiriadis, and G. Takács, Phys. Rev. Lett. **121**, 110402 (2018).
[51] I. Kukuljan, S. Sotiriadis, and G. Takács, J. High Energy Phys. 07 (2020) 224.
[52] I. Kukuljan, arXiv:2101.07807.
[53] S. Rychkov and L. G. Vitale, Phys. Rev. D **91**, 085011 (2015).
[54] S. Rychkov and L. G. Vitale, Phys. Rev. D **93**, 065014 (2016).
[55] Z. Bajnok and M. Lajer, J. High Energy Phys. 10 (2016) 050.
[56] J. Elias-Miró, S. Rychkov, and L. G. Vitale, Phys. Rev. D **96**, 065024 (2017).
[57] M. V. Berry and M. Tabor, Proc. R. Soc. A **356**, 375 (1977).
[58] R. Samajdar and S. R. Jain, J. Math. Phys. (N.Y.) **59**, 012103 (2018).
[59] See Supplemental Material at http://link.aps.org/supplemental/10.1103/PhysRevLett.126.121602 for details.
[60] M. Srdinšek, T. Prosen, and S. Sotiriadis, https://doi.org/10.5281/zenodo.4319672 (2020).